Magnetic fluctuation observation in donor-bound magnetic polarons

R. Planel, Tran Hong Nhung, G. Fishman, M. Nawrocki

HAL Id: jpa-00209838
https://hal.science/jpa-00209838

Classification
Physics Abstracts
78.20L — 75.30E — 75.30 — 72.80E

Magnetic fluctuation observation in donor-bound magnetic polarons

R. Planel, Tran Hong Nhung (*), G. Fishman and M. Nawrocki (**)

Groupe de Physique des Solides de l'Ecole Normale Supérieure (⁺),
Tour 23, 2, place Jussieu, 75251 Paris Cedex 05, France

Résumé. — On étudie la distribution énergétique des polarons magnétiques liés au donneur dans les alliages CdMnS et CdMnSe, grâce à la diffusion Raman par spin-flip. L'influence des fluctuations magnétiques sur les formes des raies est mise en évidence. On apporte aussi une preuve du superparamagnétisme des moments géants associés aux polarons magnétiques.

Abstract. — The energy distribution of donor-bound magnetic polarons is studied in CdMnS and CdMnSe alloys, using the spin-flip Raman scattering technique. The influence of magnetic fluctuations on the lineshapes is proved. Evidence of the superparamagnetism of giant moments associated to magnetic polarons is also reported.

1. Introduction.

The influence of Mn^{++} ion d-shells on delocalized electron states (band electrons) was the first stage of studies in semimagnetic semiconductors (SMSC) [1]. Then, bound magnetic polarons (BMP) were evidenced around donor or acceptor centres in these materials [2, 3]. The importance of fluctuations in these experimental observations was pointed out by Dietl and Spałek [4], and other various theoretical treatments of these effects in SMSC were stimulated [5, 6].

The aim of this paper is to present experimental results of spin flip Raman scattering (SFRS) on BMP at several temperatures and to throw some light on the influence of fluctuations by explicitly explaining the experimental lineshapes. Before going further into details we have to specify that we do not deal in this paper with the problem of acceptor centres : in that case, composition fluctuations smear out experimental results and the theoretical description of magnetic fluctuations is complicated due to the non validity of the linear approximation for the susceptibility [7, 8].

2. Experimental.

Two different wide gap semimagnetic alloys were studied : CdMnSe and CdMnS, both growing in wurtzite crystalline structure and of n-type without intentional doping. Recently, SFRS from donors has been observed in both materials [2, 5, 9-11]. We will present detailed results on $Cd_{0.95}Mn_{0.05}Se$ and $Cd_{0.85}Mn_{0.15}S$ compounds. Zero-field SFRS experiments were carried out using a standard experimental apparatus including an adjustable temperature cryostat. To get zero-field SFRS spectra with sufficient separation from the elastic scattering requires some additional precautions : in order to reduce elastic scattering, the exciting polarization was parallel to the wavevector of scattered photons (a possible scattering configuration is shown in figure 4). In addition, exciting light-energy has to be properly selected to find an optimum between the resonance effect (which increases the SFRS intensity) and the residual absorption from exciton states at higher energies. We used a CW dye-laser excitation in CdMnSe and the various lines of a CW Ar laser in CdMnS. Finally, the elastic *versus* Raman scattering ratio also depends on the overall quality of the samples, and on their proper orientation to avoid birefringence effects which alter the scattering polarization geometry. This ratio could be reduced to, roughly, 10^3 in our best CdMnSe sample. Great care has been taken to avoid heating of the donor BMP.

_____

(*) Institute of Physics, Hanoi, Viet-nam.
(**) Institute of Experimental Physics, University of Warsaw, Poland.
(⁺) Laboratoire associé au C.N.R.S.

Exciting intensity was reduced to 10^3 W/cm² in CdMnSe and 10^2 W/cm² in CdMnS which is more sensitive to laser heating as discussed in [11].

Typical spectra are shown in figures 1 and 2 for various temperatures. We now show that, as suggested in [4] these spectra essentially reflect the energetic distribution of the magnetic system.
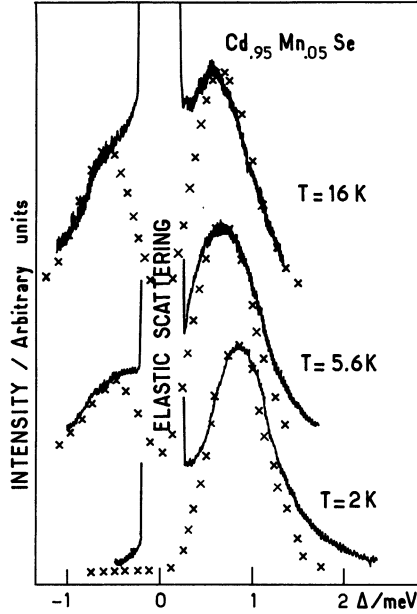

Fig. 1. — SFRS spectra in zero external field and for various temperatures, in $Cd_{0.95}Mn_{0.05}Se$. Exciting energy is 1.867 eV ($\lambda = 6\,637$ Å). Theoretical curves (×) are generated from equations (4) and (15), with $\sqrt{2}\ W_0 = 0.62$ meV and $T_{AF} = 0.6$ K.
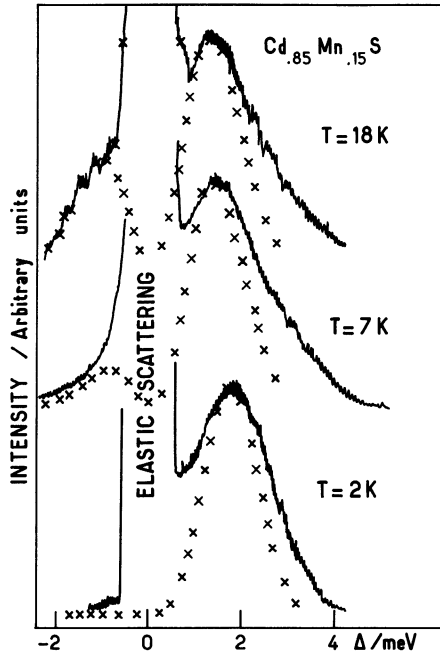

Fig. 2. — SFRS spectra in zero external field and for various temperatures, in $Cd_{0.85}Mn_{0.15}S$. Exciting energy is 2.540 eV ($\lambda = 4\,880$ Å). Theoretical curves (×) are generated from equations (4) and (15), with $\sqrt{2}\ W_0 = 1.2$ meV and $T_{AF} = 1.2$ K.

3. Simplified BMP theory.

In this section, we present a simple derivation of the BMP energy distribution. With additional hypotheses, it provides the same results as the more rigorous and extensive treatments of [4, 5].

Assuming a zero external magnetic field and independent Mn^{++} ions, the spin Hamiltonian around a donor reduces to exchange interaction between the donor electron and the Mn^{++} 5/2 spins lying in its orbit :

$$\mathcal{H}_{ex} = - \alpha \sum_i | \varphi(\mathbf{r}_i) |^2 \, \boldsymbol{\sigma}.\mathbf{S}_i \tag{1}$$

where $\boldsymbol{\sigma}$ is the spin of the donor electron, $\mathbf{S}_i$ the spin of the Mn^{++} ion located in $\mathbf{r}_i$ and $\varphi(\mathbf{r})$ the electron envelope function. α is the *mean* exchange integral since, strictly speaking, it may differ for the two cation sites in the primitive cell of wurtzite structure.

3.1 « Box » model. — Firstly, we treat the over-simplified case of a constant electronic enveloppe,

$$| \varphi(\mathbf{r}) |^2 = (\tfrac{4}{3} \pi a^3)^{-1} \theta(a - r),$$

where $\theta(a - r)$ is the step function. In fact, donor states are likely to be hydrogenic, as they are in non-magnetic semiconductors such as CdS or CdSe. However, most of the physics may be discussed using this model.

The system governed by the Hamiltonian $\mathcal{H}_{ex}$ can then be solved exactly. The eigen-energies are labelled by the quantum number J of the total momentum of the Mn^{++} spin system :

$$E_{\uparrow\uparrow}(J) = - \alpha J/2 \ [E_{\uparrow\downarrow}(J) = \alpha(J + 1)/2],$$

when the donor spin is parallel [antiparallel] to the Mn^{++} magnetization. The degeneracy of these levels may be calculated by addition of the 5/2 spins located within the « box ».

However, in the donor case of interest, the result may be very well approximated by treating the Mn^{++} spins as classical and using the Gaussian approximation for computing the density of states with a given resultant spin $\mathbf{s} = \left| \sum_{i=1}^{N} \mathbf{S}_i \right|$. This requires that $N^{-1/2} \ll 1$ and $s \ll NS$ (with $S = 5/2$) i.e. that the magnetic susceptibility may be considered as linear. In this case, the density of states may be parametrized as :

$$P(s)\,ds \propto (s^2/S^2) \exp(- 3\,s^2/2\,NS^2)\,ds \tag{2}$$

which is a well known solution of the random-walk problem [12]. The energy is written :

$$E_\sigma(s) = - (\tfrac{4}{3} \pi a^3)^{-1} \alpha \sigma s \tag{3}$$

where σ *labels* the eigenstates of the BMP : $\sigma = \pm 1/2$ depending on whether the donor spin is parallel or

antiparallel to s (let us recall that there is no particular direction in the problem, as there is in a Zeeman effect).

In an SFRS experiment, donor-BMP states with $\sigma = 1/2$ ($\sigma = -1/2$) contribute to Stokes (anti-Stokes) scattering. In other words no averaging of the donor electron spin is expected from this experiment. This is where our stand-point differs from the first paper by Dietl and Spałek [4]. Consequently the scattering event associates a shift $\Delta = -2 E_\sigma(s)$ to each donor-BMP (with the appropriate sign convention that Stokes shift is positive).

Thus, the SFRS lineshape reflects the density of states given by equations (2), (3). The energy scale differs by a factor of 2 and the density of states has to be multiplied by the Boltzmann population factor. Thus the lineshape is :

$$\mathfrak{F}(\Delta) \, d\Delta \propto \Delta^2 \exp(-\Delta^2/8 \, E_p \, kT + \Delta/2 \, kT) \, d\Delta \quad (4)$$

which takes into consideration both positive and negative Δ. In equation (4), E_p stands for « polaron energy » and connects all physical parameters of interest for the problem. In this « box » model :

$$E_p = E_p^B = (3 \, NS^2/4 \, \pi a^3) \, (\alpha^2/16 \, \pi a^3) \, (1/kT)$$
$$= 3 \, \alpha^2 \, \chi/16 \, g^2 \, \mu_B^2 \, \pi a^3 \quad (5)$$

where N is the number of Mn^{++} ions inside the « box », and thus χ is the low-field susceptibility per unit volume of these independent classical spins.

Note that other quantities may be calculated from equations (2), (3) such as the mean BMP exchange energy :

$$\langle E \rangle = (3 \, E_p \, kT + E_p^2)/(E_p + kT) \quad (6)$$

which is not obtained by SFRS measurements but may be the quantity of interest in others experiments [8]. At low temperatures $\langle E \rangle = E_p$, while at high temperatures, it vanishes as $3 \, E_p$, as expected in high temperature development.

Coming back to equation (4), it reveals the two main features due to magnetic fluctuations in BMP.

i) The most probable Stokes-shift is

$$\Delta_M = E_p + (E_p^2 + 8 \, E_p \, kT)^{1/2} \quad (7)$$

which reduces to $2 \, E_p$ at low temperatures but does not vanish as temperature increases. It tends towards the constant caracteristic value : $\lim_{T \to \infty} (8 \, E_p \, kT)^{1/2}$, which is conveniently denoted $\sqrt{2} \, W_0$ by Heiman et al. [5]. The same occurs for the most probable anti-Stokes shift. This is due to the assumption that the electron spin is quantized along the resultant magnetization inside the donor envelope function. The quantity of interest is the absolute value of this magnetization and not a particular component. In other words, the proper quantum number of the Mn^{++}

spin system for the exchange Hamiltonian (see Eq. (1)) is J and not M.

ii) The linewidth of SFRS is of the same order of magnitude, as the lineshape $(8 \, E_p \, kT)^{1/2}$, if other broadening factors may be disregarded (such as composition fluctuation broadening).

3.2 MORE GENERAL TREATMENT. — To use a more realistic description of the donor envelope function, we have to show that equation (4) may be written :

$$\mathfrak{F}(\Delta) \, d\Delta \propto \exp(-F_\sigma(\Delta)/kT) \, d^3\Delta \quad (8)$$

where $F_\sigma(\Delta)$ is the Landau free energy functional of the Mn^{++} spin system, submitted to a Zeeman-like interaction in the BMP direction. Following Dietl and Spałek [4], we may write :

$$F_\sigma(\Delta) = \int \left[-\mathbf{M}(\mathbf{r}).\mathbf{H}(\mathbf{r}) + \frac{1}{2\chi} M^2(\mathbf{r}) \right] d^3r \quad (9)$$

where $\mathbf{M}(\mathbf{r})$ is the local magnetization and $\mathbf{H}(\mathbf{r})$ the local exchange-equivalent field, both being parametrized as a function of « spin-splitting vector » $\mathbf{\Delta}$. In the « box » model :

$$\mathbf{M}(\mathbf{r}) = (g\mu_B/\alpha) \, \mathbf{\Delta}\theta(a - r) \quad (10a)$$

$$\mathbf{H}(\mathbf{r}) = (3 \, \alpha/4 \, g\mu_B \, \pi a^3) \, \mathbf{\sigma}\theta(a - r) \quad (10b)$$

which rapidly becomes

$$F_\sigma(\Delta) = -\mathbf{\Delta}.\mathbf{\sigma} + \Delta^2/8 \, E_p^B . \quad (11)$$

However, the transition from equations (11) to equations (8) and (4) is far from obvious in the general case, although it may be grounded on common sense arguments [4]. It requires rigourous justification such as those in [4, 5] and also depends on the validity of Gaussian approximation for the susceptibility (see a more general discussion in [8]).

We shall consider in the following that we remain in the validity range of Gaussian approximation, which allows us to use the Landau free-energy functional approach and thus to generalize equations (10) to any form of the envelope-function.

Using a hydrogenic-type donor envelope function, Dietl and Spałek derived equation (11), with E_p^B replaced by :

$$E_p^H = \alpha^2 \, \chi/32 \, g^2 \, \mu_B^2 \, \pi a_H^3 = E_p^B(a_H)/6 \quad (12)$$

where a_H is now the donor Bohr radius.

The numerical coefficient between E_p^H and E_p^B comes from the ratio : $\int \varphi_H^4(r) \, d^3r \Big/ \int \varphi_B^4(r) \, d^3r$, which is the only quantity depending on the precise envelope function in this model. It may be useful, with respect to that problem, to define an effective « box » radius a_e which provides the same characteristic polaron energy in the box model as with a

different envelope type (see Table I). A comparison of this type has been done by Ryabchenko and Semenov [13] using a different starting point.

Table I. — *Effective radius a_e for different donor state wavefunctions $\varphi(r)$. The case of the «box» wavefunction is taken as standard. Comparison is made with analogous quantity R obtained by Ryabchenko and Semenov (Ref. [13]), who used a variational technique.*

$\psi(r)$	a_e/a (this work)	R/a (from R.S.)
$(4\pi a^3/3)^{-1/2}\,\theta(a-r)$	1	1
$(\pi a^2/2)^{-3/4}\,\exp[-(r/a)^2]$	$(3\sqrt{\pi}/4)^{1/3} = 1.099$	1.043
$(\pi a^3)^{-1/2}\,\exp(-r/a)$	$6^{1/3} = 1.817$	1.836

To conclude this section, we point out that equations (6) and (7) also hold for a hydrogenic-type envelope-function, with $E_p = E_p^H$ as given by equation (12).

4. Comparison with experiment.

Writing the characteristic quantity E_p as a function of susceptibility allows us to account for the antiferromagnetic interaction between Mn^{++} spins, which results in a somehow modified paramagnetic behaviour (forgetting spin-glass effects which may be observed at concentrations greater than, about, 20 % [1]).

On the one hand, high field magnetization data may be described by [14]

$$\langle S_z \rangle = S_0\, B_{5/2}[H/(T + T_0)] \qquad (13)$$

where S_0 is smaller than the ideal paramagnetic saturation value, $S = 5/2$, and T_0 is an effective positive temperature.

On the other hand, low-field susceptibility measurements may fit the empirical relation

$$\chi(T) \propto (T + T_{AF})^{-1} \qquad (14)$$

where T_{AF} is an effective temperature which differs from T_0 (see for example the results concerning $Cd_{0.977}Mn_{0.023}S$ in [10]).

Assuming now a hydrogenic donor envelope-function as the most reasonable choice for shallow impurities in wide-gap semiconductors, we write from equation (11), (13) and (14) :

$$E_p = E_p^H = \alpha^2\, \chi/32\, g^2\, \mu_B^2\, \pi a_H^3$$
$$= [S(S + 1)/12]\,(N_0\,\alpha)^2\,(xS_0/S)\,(8\,\pi a_H^3\, N_0)^{-1} \times$$
$$\times\, [k(T + T_{AF})]^{-1}$$
$$= W_0^2/4(T + T_{AF}) \qquad (15)$$

with $S = 5/2$, and where all parameters might be obtained by complementary experiments. Notice in particular that (xS_0/S) can be interpreted as an effective concentration and is deduced from high field magnetization measurements; N_0 is the number of cation sites per unit volume; $N_0\,\alpha$ is the exchange parameter deduced from conduction band spin splitting under an external field, $\Delta_0 = N_0\, \alpha x \langle S_z \rangle$, and is not very dependent on Mn concentration in a given series of compounds [1]; $(8\,\pi a_H^3\, N_0)$ is the effective number of cation sites lying under the donor electron wave function.

To discuss our results, we proceed as follows. We plot the experimental maximum of zero field SFRS line as a function of temperature and fit it to equation (7) with E_p given by equation (15). This fit depends on two independent parameters : $\sqrt{2}\,W_0$ and T_{AF}. The results are shown in figure 3. Experimental results are restricted to a temperature range below 20 K for CdMnSe and 30 K for CdMnS, due to the decrease of zero field SFRS because of ionization of donors. As we shall see, in these high temperature regions, the quantity E_p is much smaller than $(8\,E_p\, kT)^{1/2}$ and the ratio $T/(T + T_{AF})$ is close to 1. Thus we get rather unambiguously the limiting value $\sqrt{2}\,W_0$. Then, the low T region is fitted by adjusting T_{AF}.
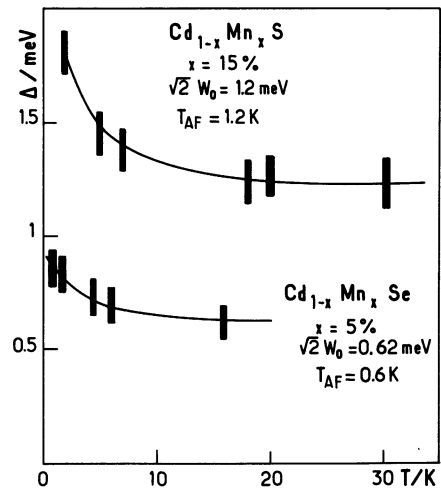
Fig. 3. — SFRS Stokes-energy in zero external field *versus* temperature, for $Cd_{0.85}Mn_{0.15}S$ and $Cd_{0.95}Mn_{0.05}Se$. The solid curves are obtained from equation (7) in the text with two adjusting parameters : $\sqrt{2}\,W_0$ and T_{AF}.

From the experimental determination of $\sqrt{2}\,W_0$, it is possible to extract, for example, a measurement of the Bohr radius, independently from the donor binding energy. These data, and the parameters used, are gathered in table II for both materials. Main uncertainties lie in the determination of the exchange energy $N_0\,\alpha$ and the effective concentration $(xS_0/2.5)$. They may be estimated to 10 % each, which results in a 10 % uncertainty on the Bohr radius determi-

Table II. — *Parameters used in this work.* $\sqrt{2}\,W_0$ *and* T_{AF} *are determined by experiments presented here ; Bohr radii are deduced, using in addition* $(xS_0/2.5)$ *and* $N_0\,\alpha$.

Quantity	Symbol	Sample	Sample	Unit
Material		CdMnSe	CdMnS	
Cation Site Density	N_0	1.77×10^{22} a)	2×10^{22} b)	cm^{-3}
Mn concentration (technologic)	x	5%	15%	
High temperature BMP-splitting	$\sqrt{2}\,W_0$	0.62	1.2	meV
Antiferromagnetic temperature	T_{AF}	0.6	1.2	K
Effective concentration	$xS_0/2.5$	2.7% c)	4.3% e)	
Exchange parameter	$N_0\alpha$	0.26 d)	0.22 e)	eV
Bohr radius	a_H	39.5	25.5	Å

(a) CdSe value.
(b) CdS value.
(c) From Dietl and Spałek, reference [4].
(d) From Heiman et al., reference [5].
(e) Data obtained from the same sample, from Nawrocki et al., reference [11].

nation. However, our determinations of Bohr radii are in remarkable agreement with values generally admitted from donor binding energy in CdS and CdSe.

These two parameters, $\sqrt{2}\,W_0$ and T_{AF} being obtained, theoretical lineshapes may be derived from equation (4), with $E_p = E_p^H = W_0^2/4(T + T_{AF})$. They are compared to experimental results, without any further adjustment, in figures 1 and 2.

This comparison is quite illustrative for intermediate temperatures. At lower T, no antiStokes line may be detected ; at higher T, the scattering intensity reduces as the donors ionize, and no clear maximum may be observed on a broad symmetric background. These intermediate temperatures are typically lower in CdMnSe ($\sim$ 6 K) than in CdMnS ($\sim$ 16 K) since the donor ionization energy and BMP effects are larger in this latter material.

In CdMnSe, with $x = 5\%$, the Stokes and anti-Stokes linewidths are fairly well accounted for by magnetic fluctuations alone. Note that in an external field, the composition fluctuations cannot be neglected any more. In the same material, we found (see Ref. [2]) that the linewidth amounts to 0.8 meV in 2 tesla. Since the magnetic fluctuation broadening should reduce as the susceptibility (see equation (16) below), we may estimate it to be 0.4 meV in such an external field. Consequently the composition broadening should reach about 0.7 meV for a 12 meV Stokes-shift. It is worth noticing that such an order of magnitude may be explained by a random distribution of some 300 Mn^{++} ions in the donor orbit finite volume.

In CdMnS with $x = 15\%$, which seems to be poorer quality material, the magnetic fluctuations only account for part ($\sim$ 1.5 meV) of the total broadening ($\sim$ 2.5 meV). This order of magnitude remains unchanged in an external field, as found in [11], which excludes inhomogenous broadening due to composition fluctuations. Thus the linewidth should be explained by more complicated effects.

5. BMP alignment.

We now present a complementary experiment which evidences the alignment of BMP, that is of the local magnetization, along a weak external field.

The experiment makes use of SFRS polarization selection rules [15]. Let us just recall that, in CdMnSe, the main possible virtual intermediate states are the donor-bound exciton states I_{2A} and I_{2B} which are built with holes from the two upper valence bands A and B. As a matter of fact, large spin-orbit coupling lowers the C-exciton state contribution. Among several possible, we chose the scattering configuration, shown in figure 4, $X(Z, \pm)\,Z$. Exciting polarization is parallel to the c-axis and magnetic field direction (referred to as the z direction), and scattering is collected along the same z direction, with selection of the circular polarizations (referred to as σ^+ and σ^-).
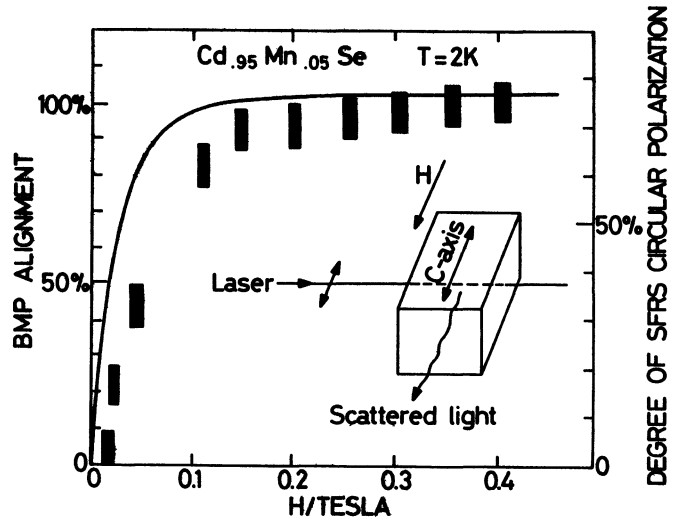

Fig. 4. — BMP alignment along external field H. The solid curve is obtained from equation (17) as explained in the text, without adjusting parameter.

Let us consider a donor BMP with local quantization direction defined by the usual polar angles θ and φ. On the one hand, the virtual intermediate states from the A valence band should not contribute to the scattering, since there is no P_z-symmetry component in the A-hole wave function. On the other hand, the I_{2B}^+ (I_{2B}^-) state only contributes to σ^+ (σ^-) scattering.

These two contributions are governed by the quantization of the donor low-energy state along the z direction : $\cos(\theta/2)\,|\downarrow\rangle + \sin(\theta/2)\,|\uparrow\rangle$. Consequently the degree of polarization $(\sigma^+ - \sigma^-)/(\sigma^+ + \sigma^-)$ of SFRS from donor-BMP with local spin splitting

axis (θ, φ) is proportional to $(\cos^4 \theta/2 - \sin^4 \theta/2)/$ $(\cos^4 \theta/2 + \sin^4 \theta/2)$. Thus the experimental degree of polarization measures the quantity : $2 \langle \cos \theta \rangle /$ $(1 + \langle \cos^2 \theta \rangle)$, averaged over all BMP's. It should tend towards 1 in large external fields.

5.1 DISCUSSION OF THE RESULTS. — The experiment was done in $Cd_{0.95}Mn_{0.05}Se$, at $T = 2$ K. This material is best suited for selection rule studies, due to the large spin orbit coupling. Exciting polarization and energy were adjusted to optimize the high field circular polarization of scattered light, but the alignment of the c-axis and magnetic field was not easy to achieve perfectly in our set up. We found the circular degree of polarization to be, at most, 0.75 for exciting energy 1.83 eV.

We checked that such a discrepancy is not due to the giant spin-splitting of the I_{2B} level, which cannot be neglected with regard to the energy denominator and thus increases the σ^- efficiency. However, this effect accounts only for a few per cent of the depolarization at the exciting energy we used.

To explain this imperfect polarization, it is to be noticed that our experiment is very sensitive to the perfect alignment of c-axis and magnetic field directions. The first reason is birefringence, since we had to work in right angle scattering and light travels through, typically, 1 mm thickness material. The second reason is easier to evaluate quantitatively : it is rapidly shown that the I_{2A} virtual state contribution is, when allowed, greater by one order of magnitude than the I_{2B} contribution which provides circular polarization (this is mainly due to smaller energy denominator). As a consequence, misalignment by one or two degrees increases unpolarized scattering to values comparable with the polarized scattering. We conclude that the 0.75 experimental value of circular degree of polarization may be reasonnably considered as a maximum and should correspond to alignment of all BMP's along the external field.

5.2 THEORY. — We now estimate the variation of $\langle \cos \theta \rangle$ and $\langle \cos^2 \theta \rangle$ as a function of external field. The simplified approach presented in part 3.2 may be generalized, with the same fundamental assumptions and limitations, to include action of an external field in the Landau functional.

Following Dietl and Spałek [4], we define the « spin splitting vectors » Δ and Δ_0. The length of Δ is the electron spin splitting and its direction lies along the local quantization axis of the BMP. The same definitions hold for Δ_0 when no fluctuation or polaron effects are taken into account; thus Δ_0 is the conduction band spin splitting under the influence of mean magnetization M_0.

It follows that equation (4) is easily generalized [4] :

$$\mathcal{F}(\Delta) \, d^3\Delta \propto \Delta^2 \, \exp[-(\Delta-\Delta_0)^2/8 \, E_p \, kT + \Delta/2 \, kT] \times$$
$$\times \, d\Delta \, d \cos \theta \, d\varphi \quad (16)$$

which only depends on θ through

$$\mathcal{F}(\Delta) \propto \exp(2 \, \Delta\Delta_0 \cos \theta/8 \, E_p \, kT) \, .$$

We deduce that, for any Stokes-shift :

$$\langle \cos \theta \rangle = L(X) = L(2 \, \Delta\Delta_0/8 \, E_p \, kT)$$

where $L(X)$ is the Langevin function, commonly used to describe the magnetization m of N classical independent moments : $m = N\mu L(\mu H/kT)$, with $L(X) = \coth(X) - 1/X$.

In the same way, one easily show that : $\langle \cos^2 \theta \rangle =$ $1 - 2 \, L(X)/X$, so that the degree of polarization should be :

$$(\sigma^+ - \sigma^-)/(\sigma^+ + \sigma^-) = L(X)/[1 - L(X)/X] \quad (17)$$

with $X = 2 \, \Delta\Delta_0/8 \, E_p \, kT$.

We know interprete the argument X using :

$$\Delta_0 = N_0 \, \alpha(xS_0/S) \, [S(S+1) \, g\mu_B \, H/3 \, k(T+T_{AF})]$$
$$(18)$$

which is easily deduced from equations (13), (14) and assumes a small external field. In addition, we define a mean Mn^{++} spin value $\bar{S}$ inside the BMP through

$$\Delta = N_0 \, \alpha(xS_0/S) \, \bar{S} \, . \quad (19)$$

Remembering (xS_0/S) is the effective Mn concentration and E_p is given by equation (15), we get :

$$2 \cdot \Delta\Delta_0/8 \, E_p \, kT = 8 \, \pi a_H^3 \, N_0(xS_0/2.5) \, g\mu_B \, H\bar{S}/kT$$
$$= N_e \, g\mu_B \, H\bar{S}/kT \quad (20)$$

where N_e is the effective number of Mn^{++} ions inside the sphere of radius a_e, which is the effective radius defined in section 3 (see Table I).

This expression of the Langevin function argument provides a clear physical interpretation of equation (17). The variation of $\langle \cos \theta \rangle$ expresses the alignment of a giant classical spin $N_e \, \bar{S}$ under the external field (16).

For external fields smaller than 0.1 T, the BMP spin splitting is roughly constant [2] and equal to 0.8 meV at $T = 2$ K; thus, from numerical values in table II, we easily estimate $\bar{S} \sim 0.11$ and $N_e \sim 740 \, Mn^{++}$ ions.

The BMP may be thought of as bearing a giant spin $\bar{S}N_e \sim 81$, to be compared to 2.5, the spin value for isolated Mn^{++} ions.

As the field is increased, $\bar{S}$ also increases and may be deduced from experimental Δ through equation (19). It results in a rapid alignment of BMP along the field. Expected values of the polarization ratio are thus plotted in figure 4 and compared to experimental results. The qualitative agreement is good, remembering we have assumed that the saturation value $\langle \cos \theta \rangle = 1$ corresponds to 0.75 degrees of circular polarization. The main feature to be noticed is the order of magnitude of the saturation field, which is

around 0.1 tesla, to be compared with the saturation field of isolated ions, typically 2 tesla in $T \sim 2$ K. This experiment may be related to the variation of $\Delta_M(H)$ for small H, which was also understood in terms of « giant spin » alignment [2, 5].

6. Conclusion.

To conclude, we point out the good agreement between our experimental results and a BMP theory which accounts for magnetization fluctuations. Such a theory explains SFRS linewidths, especially in the case of the CdMnSe samples we studied. Even more convincing are the SFRS line shapes in the interme-

diate temperature region, which are quite consistent with a density of state which is minimum at zero energy. This is predicted by a simple statistical approach based on the random-walk problem. Finally, we presented experimental evidence of the « giant spin » effects associated with BMP.

References

[1] See for example the recent review papers by :
Gaj, J., Ref. [3] p. 797.
Grynberg, M., Ref. [7] p. 461.

[2] Nawrocki, M., Planel, R., Fishman, G. and Ga-łazka, R., Ref. [3] p. 823 ; Phys. Rev. Lett. 46 (1981) 735.

[3] Golnik, A., Gaj, J., Nawrocki, M., Planel, R. and Benoit à la Guillaume, C., Proceedings of the XVth Int. Conf. Physics of Semiconductors, Kyoto, 1980 (J. Phys. Soc. Jpn. Suppl. A 49 (1980) 819.)

[4] Dietl, T. and Spałek, J., Phys. Rev. Lett. 48 (1982) 355 ; Phys. Rev. B 28 (1983) 1548.

[5] Heiman, D., Wolff, P. A. and Warnock, J., Phys. Rev. B 27 (1983) 4848.

[6] Mauger, A., Phys. Rev. B 27 (1983) 2308.

[7] Tran Hong Nhung and Planel, R., Proc. of the XVIth Int. Conf. Phys. Semicond., Montpellier, 1982 ; Physica 117B-118B (1983) 488.

[8] Tran Hong Nhung, Planel, R., Benoit à la Guillaume, C. and Bhattacharjee, A. K., to be published.

[9] Alov, D. D., Gubarev, S. I., Timofeef, V. B., Shepel, B. N., Pis'ZhETF 34 (1981) 76 — (JETP Lett. 34 1981, 71.)

[10] Heiman, D., Shapira, Y. and Foner, S., Solid State Commun. 45 (1983) 899.

[11] Nawrocki, M., Kozielski, M. J., Mollot, F. and Planel, R., to be published in Phys. Status Solidi.

[12] Watson, G. N., Theory of Bessel Functions (ed. Cambridge Univ. Press) 1966, p. 419.

[13] Ryabchenko, S. M. and Semenov, Yu. G., Zh. ETF 84 (1983) 1419 (Sov. Phys. JETP 57 (1983) 825).

[14] Gaj, J., Planel, R. and Fishman, G., Solid State Commun. 29 (1979) 435.

[15] For a treatment of SFRS selection rules in wurtzite structure, see for example. Thomas, D. G. and Hopfield, J. J., Phys. Rev. 175 (1968) 1021.

[16] Analogous experiment has been recently published in CdMnS by Alov, D. L., Gubarev, S. I. and Timofeev, V. B., Zh. ETF 84 (1983) 1806 (Sov. Phys. JETP 57 (1983) 1052). The results are interpreted in terms of giant spin alignment.